Atomistic and Flory−Stockmayer Analyses of Irradiated i-PP Gel Fractions and Comparison with Results from PE

R. A. Jones,*,† J. I. Cail,‡ R. F. T. Stepto,‡ and I. M. Ward†

IRC in Polymer Science and Technology, Department of Physics, University of Leeds, Leeds LS2 9JT, U.K.; and Polymer Science and Technology Group, Manchester Materials Science Centre, University of Manchester and U.M.I.S.T., Grosvenor St., Manchester M1 7HS, U.K.

Received April 20, 2000; Revised Manuscript Received July 5, 2000

ABSTRACT: Atomistic computation and Flory−Stockmayer (F−S) theory have been successfully applied to the analysis of gel fraction data from a microporous isotactic poly(propylene) (i-PP), irradiated and annealed in the presence of acetylene. The presence of linearly propagating chain reactions is demonstrated by the computed maximum possible gel−radiation dose curves (in the absence of scissions and chain reactions), being initially much smaller than the experimental gel fraction curve. Both analyses are carried out in terms of the number of "gel-effective" chain steps ($N_{CS,D}$) per initiating radical at a given dose (D). The results are in keeping with two similar previous studies by the authors, on data from two different linear low-density poly(ethylene)s (LLDPEs), one of which had been conducted both in vacuo and in acetylene. With the exception of one LLDPE, the maximum $N_{CS,D}$ values ($(N_{CS,D})_{max}$), and nth order decreases of $N_{CS,D}$ with respect to dose, derived by the two methods for both polyalkenes in all three studies, are in close agreement. For reasons described, the nth order decrease rate constants from the two analyses differ by an order of magnitude, but follow the same trends. $(N_{CS,D})_{max}$ decreases with increasing preirradiated molecular weight of the polyalkenes, under equivalent conditions, because a smaller $N_{CS,D}$ is required to produce a given gel fraction. Both analyses demonstrate that all the gel fraction vs number of "gel-effective" cross-links per preirradiated molecule ($(N_{Xeff,D}/N_M)_{gel}$) curves conform to a universal function, irrespective of the initial degree of polymerization, or the irradiation and annealing conditions used to produce them. The universalities of the gel fraction vs $(N_{Xeff,D}/N_M)_{gel}$ curves, are demonstrated in terms of the number- and weight-average preirradiated molecular weights in the atomistic and F−S methods, respectively. This work paves the way to the simulation and characterization of gel fraction data to give the numbers of cross-links and scissions required to reproduce rheological data.

Introduction

Previously, the application of atomistic and Flory−Stockmayer (F−S) analyses of gel fractions has proved successful in demonstrating the presence of chain reactions in LLDPEs, irradiated both in the presence of acetylene and in vacuo.[1] For given irradiation conditions, both analytical techniques showed similar $N_{CS,D}$ values per initiating radical at a given dose (D), and also similar orders of decay of $N_{CS,D}$ with respect to dose. From the atomistic analysis, at a given dose, the average number of "gel-effective" cross-links required to produce the gel fraction per preirradiated number-average chain $(N_{Xeff,D}/N_M)_{gel}$ was calculated. $N_{Xeff,D}$ is the number of "gel-effective" cross-links per kg at dose D, and N_M is the number of initial chains of number-average kg molecular weight $M_{n,0}$. Following this, a rheology study, based on melt relaxation moduli at long times, of an LLDPE irradiated in the presence of acetylene, yielded "total" numbers of permanent cross-links, at given doses per preirradiated number-average chain ($(N_{X,D}/N_M)_{rh}$), where $N_{X,D}$ is the number of permanent cross-links per kg at dose D.[2] At low gel fractions (<0.4), $(N_{X,D}/N_M)_{rh}$ was found to be almost equal to $(N_{Xeff,D}/N_M)_{gel}$ in the same LLDPE samples. That is to say "total" and "gel-effective" numbers of cross-links were nearly identical and all the cross-links increased the molecular weight of the irradiated polymer. Since initially intramolecular redundancies are of low probability and scissions are not likely to be in the same molecules as cross-links, this corroborated the premise of the atomistic model, that above some limiting $M_{n,0}$, only one cross-link, between two previously unlinked molecules, was required to increase the gel fraction. From gel fractions of 0.4 onward, the $(N_{X,D}/N_M)_{rh}$ vs $(N_{Xeff,D}/N_M)_{gel}$ curve diverges, because $(N_{X,D}/N_M)_{rh}$ represents the total number of cross-links including redundancies and the extra cross-links required to overcome scission processes. As far as gel fraction 0.8, a least-squares fit of the $(N_{X,D}/N_M)_{rh}$ vs $(N_{Xeff,D}/N_M)_{gel}$ data conformed to a power function

$$\left(\frac{N_{X,D}}{N_M}\right)_{rh} = \left(\frac{N_{Xeff,D}}{N_M}\right)_{gel} + \frac{q}{2}\left(\frac{N_{Xeff,D}}{N_M}\right)_{gel}^{q} \qquad (1)$$

where q was approximated to the integer value 4. The rapid rise in $(N_{X,D}/N_M)_{rh}$ with respect to $(N_{Xeff,D}/N_M)_{gel}$, above gel fraction 0.4, results from the increasing redundancy of "total" cross-links to augment the average molecular weight. Part of this redundancy arises from the increasingly smaller probability that new cross-links will repair chain scissions as the gel fraction approaches unity. Hence, a massive redundancy begins in the ability of cross-links to increase the gel fraction. The power relationship of eq 1 could not be verified beyond gel fraction 0.8, because moduli saturation significantly affected $(N_{X,D}/N_M)_{rh}$. Acetylene was used in these studies, because it significantly reduced main chain scission processes and made measurements possible over almost the entire range of gel fractions. The use of acetylene does not limit the validity of the results, because the gel fraction vs $(N_{Xeff,D}/N_M)_{gel}$ curves from LLDPEs are nearly identical, irrespective of the irradiation condi-

* To whom correspondence should be addressed.
† University of Leeds.
‡ University of Manchester and U.M.I.S.T.

10.1021/ma000701g CCC: $19.00
Published on Web 08/25/2000

tions used to produce them.[1,2] Significantly, the gel fraction vs $(N_{Xeff,D}/N_M)_{gel}$ curves are also independent of the initial preirradiated $M_{n,0}$ (ca. 22.05 and 30.50 kg mol^{-1}). In addition, the decays of $N_{CS,D}$ with respect to dose, demonstrated by both analytical techniques, in the presence of acetylene and in vacuo, are indicative of free-radical initiated, linearly propagating, chain-reaction systems, in which $N_{CS,D}$ decreases successively toward higher doses as a result of more frequent radical−radical termination reactions caused by increased concentrations of radicals. Since structure is accounted for in the determination of $N_{CS,D}$ it was proposed that chain reactions, rather than polydispersity, explain most of the deviation from Charlesby−Pinner behavior in irradiated polyalkanes.[3]

It can be concluded from these studies that both the atomistic and F−S approaches afford simple and convenient methods of analysis of radiation-induced gel fractions, providing additional insight as to the composition of the irradiated polymers. Since the atomistic $(N_{Xeff,D}/N_M)_{gel}$ curves from the two LLDPEs were nearly identical, irrespective of the irradiation conditions and their initial $M_{n,0}$ (probably above some lower limiting $M_{n,0}$), the possibility that they represent a universal curve, at least for alkyl polymers, is suggested. It must be stressed that this is probably not necessarily true for the gel fraction vs $(N_{X,D}/N_M)_{rh}$ curves of different alkyl polymers, but that they can easily be related to the atomistic $(N_{Xeff,D}/N_M)_{gel}$ curves by relaxation modulii.[2] It is therefore of interest to apply the atomistic and F−S analyses to data from another alkyl polymer, to probe the possible universality of gel fraction vs $(N_{Xeff,D}/N_M)_{gel}$ curves. To this end we have chosen polypropylene in its isotactic form, (i-PP).

Experimental Section

Materials. i-PP films were provided by Hoechst-Celanese (CELGARD 2400 microporous membrane film, thickness 0.0275 mm, $M_{n,0} = 5.710 \times 10^1$ kg mol^{-1}, $M_{w,0} = 4.710 \times 10^2$ kg mol^{-1}, melting point = 168 °C, melt flow index = 1.5). Microporous films were used, because insufficient acetylene impregnation was found in earlier experiments with PP samples, due to poor diffusion characteristics. The samples were evacuated of air gases, electron beam irradiated (18 °C, dose rate = 95.24 Gy s^{-1}), and annealed (135 °C) in acetylene (ca. 1013×10^5 Pa), as per the method previously described for LLDPE.[4] It must be stressed that, to minimize oxidative degradation, the i-PP samples were not allowed to come into contact with air until annealing was complete.

Gel Fractions. Determinations were carried out on i-PP samples (0.15 ± 0.025 g), placed in steel gauze (120 gauge) containers, subjected to solvent extraction in decahydronaphthalene (decalin, 192 °C for 48 h), and then cleaned in boiling acetone (61 °C), dried and weighed as per the method described for LLDPE.[4]

Results and Discussion

1. Atomistic Analysis of Gel Fraction Curves. 1.1. Computer Generation of $(gel)_{T_{max}}$ Curves. The $(gel)_{T_{max}}$ curves represent the hypothetical maximum gel-fraction obtainable at any given dose, under the ideal conditions where only interchain radical−radical termination reactions occurred, with no chain reactions, scissions, or cross-link redundancies with respect to preirradiated chains.[3] Reactions of radical-pairs were modeled in an amorphous i-PP macro-cell (MSI, Insight II, Version 400, Amorphous Cell 6.1),[5] using the method described previously for LLDPE,[1,6] but with the following changes required for i-PP. It was necessary to use small chains of 102 carbon atoms (34 monomers) to prevent unnaturally high degrees of self-wrapping from occurring in the cells. Thirty chains were packed amorphously into unit subcells at a density of ca. 0.90 g.cm^{-3} and equilibrated for 4000 molecular dynamics steps at 293 K. A macro-cell (85.93 Å) was then constructed from 8 interlocking unit subcells and, hence, contained 240 chains and 24 480 carbon atoms (16 320 backbone carbon atoms), or 73 920 atoms in total. The use of small chains necessitated the introduction of scaling factors to increase the number of monomers per chain to those of the i-PP being modeled. The validity of this approach was checked previously with LLDPE.[1] After the number of atoms was scaled by a factor of 39.91, the effective number of atoms in the simulations of the 0.0275 mm microporous i-PP film was 2.950×10^6. Although, i-PP is a polycrystalline material, the amorphous macrocell was assumed to be suitable for the experiments, because the atomistic analysis only requires the cell for the production of $(gel)_{T_{max}}$ curves and maximum gel-fractions can only be obtained in amorphous systems. Also, it is believed that the cross-links in the crystalline regions of i-PP will be confined to the lamellae fold−surface interfaces, similar to the case of PE,[7] possibly as a result of radical migration.[8] In addition, acetylene does not alter the balance of cross-links between the amorphous and crystalline regions, because it does not penetrate the latter.

Radicals were generated using a simple H atom ejection model, which had previously been tested and found to be an effective radical-pair generator in simulations using amorphous i-PP macrocells.[9] All primary initiating radicals (r_i) were generated at random on "b'-type carbon atoms ($\sim C^aH_2C^bHC^cH_3\sim$), because it was demonstrated in the generator study that initiating radicals are predominantly of this type. For each initiating radical, subsequent partner radicals (r_p) were selected randomly from the total number of all types of available pairs assigned to that radical by the generator. An array of the selected (r_i) and (r_p) radicals was made in the computer, and the (r_i) radicals were cross-linked with the spatially nearest radical ((r_i) or (r_p)), which, except at very high doses, was the corresponding (r_p) partner-radical. One cross-link between two chains, which were previously unlinked, was considered to be the criterion for raising the molecular weight. This has been shown to be true for an LLDPE, by interpretation of rheologically determined relaxation modulii in the melt,[2] assuming that the initial $M_{n,0}$ was above a certain value. The gel fraction (g) at dose (D) was considered to be the sum of the cross-linked chains (j) divided by the sum of all the initial chains (k) in the scaled amorphous macro-cell ($g_D = \Sigma(j)/\Sigma(k)$).

The position and shape of the theoretical $(gel)_{T_{max}}$ curves in alkyl polymers depend largely on the number of radicals ($N_{R,D}$/mol-spins J^{-1}) at a given absorbed dose (D/(Gy or J kg^{-1})), the dose in its relationships to other environmental effects, and the preirradiated $M_{n,0}$

$$(gel)_{T_{max}} = F\left(\frac{N_{R,D}}{2}, D, M_{n,0}\right) \quad (2)$$

where $N_{R,D}$ is evaluated from the dose and the radiation efficiency value for the production of alkyl radicals $G(R^\bullet)$ (mol-spins kg^{-1})

$$N_{R,D} = DG(R^\bullet) \quad (3)$$

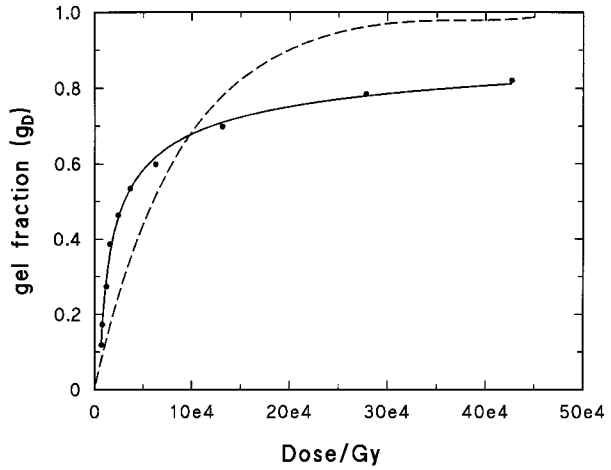

Figure 1. Gel fraction vs dose for microporous i-PP (**3a**) (CELGARD 2400, $M_{n,0} = 57.10$ kg mol^{-1}, ca. 0.0275 mm thick, in C_2H_2) (—●), together with the corresponding $(gel)_{T_{max}}$ curve for $G(R^{\bullet}) = 2.33 \times 10^{-7}$ mol spins J^{-1} (– –).

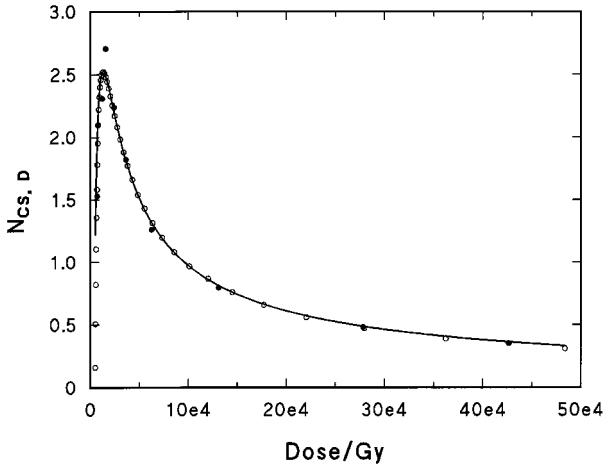

Figure 2. $N_{CS,D}$ vs dose for microporous i-PP (**3a**) ($M_{n,0} = 57.10$ kg mol^{-1}, ca. 0.0275 mm thick, in C_2H_2): experimental data (●), interpolated data (○), and functional fit to interpolated data (—).

The only $G(R^{\bullet})$ value found in the literature for PP is provided by Ohnishi et al.,[10,11] who report a value of 6.2 radicals/100 eV (or $G(R^{\bullet},PP_{Ohnishi}) = 6.43 \times 10^{-7}$ mol spins J^{-1}). However, this value is implausibly high, which is hardly surprising because there was a tendency to overestimate $G(R^{\bullet})$ values in earlier years, due to the presence of chain reactions and unresolved peaks in ESR spectra. In fact, Ohnishi et al., also quote a value for PE in the same paper of 6.4 radicals/100 eV (or $G(R^{\bullet},PE_{Ohnishi}) = 6.64 \times 10^{-7}$ mol spins J^{-1}), which is known to be wrong, in that Ichikawa et al.[12] have more recently, and reliably, determined a value of $G(R^{\bullet},PE_{Ichikawa}) = 2.40 \times 10^{-7}$ mol spins J^{-1}, utilizing the electron-spin echo (ESE) technique on samples of medium-density PE ($\rho = 0.963$ g cm^{-3}). Since the $G(R^{\bullet},PP_{Ohnishi})$ and $G(R^{\bullet},PE_{Ohnishi})$ values are so close, it is possible, for the purposes of this study, to make an estimate for the true $G(R^{\bullet},PP_{estimate})$ by scaling them to the $G(R^{\bullet},PE_{Ichikawa})$ value:

$$G(R^{\bullet},PP_{estimate}) = GR(R^{\bullet},PE_{Ichikawa})\frac{GR(R^{\bullet},PP_{Ohnishi})}{GR(R^{\bullet},PE_{Ohnishi})} \quad (4)$$

The scaling yields a $G(R^{\bullet},PP_{estimate})$ of 2.33×10^{-7} mol spins J^{-1}, which was used to generate the $(gel)_{T_{max}}$ curves in this study.

1.2. Analysis of Gel Fraction Curves Using $(gel)_{T_{max}}$ Curves. Since the $(gel)_{T_{max}}$ curve represents the maximum possible gel fractions obtainable from terminations alone, gel fractions greater than $(gel)_{T_{max}}$ can only be formed from linear (nonbranching) chain reactions, in which cross-links are also formed prior to those that are formed during the termination reactions.[1] The gel fraction results for the microporous i-PP film, irradiated and annealed in the presence of acetylene (**3a**), are shown as a function of dose in Figure 1. The experimental gel curve is initially greater but finally lower than the $(gel)_{T_{max}}$ curve, estimated using $G(R^{\bullet},PP_{estimate}) = 2.33 \times 10^{-7}$ mol spins J^{-1}, indicating that chain reactions occurred during irradiation and annealing, resulting in the production of cross-links and main-chain scissions, both of which help to define the dose-related resultant increasing molecular weight. The additional cross-links produced in the linear chain reactions, before termination reactions take place, are therefore, responsible for the initial gel fractions being higher than $(gel)_{T_{max}}$, while the scissions are responsible for the gel fractions at higher doses being lower than $(gel)_{T_{max}}$. Usually, in the absence of acetylene, much larger doses (ca. 50×10^4 Gy) are required before the dose to incipient gelation (D_g) is reached and the effects of significant levels of cross-linking begin to show.[13] In the presence of acetylene, the gel fraction (g_D) vs dose (D) curve of the microporous i-PP film gave a D_g of ca. 0.38×10^4 Gy, when extrapolated to zero using a modification of the Wanxi equation[1,14]

$$g_D = \frac{(1 - LD^{(\beta-1)}) + \sqrt{(2L^{(\beta-1)} + 1)}}{2} \quad (5)$$

where L is a constant related to the ratio of the radiation efficiency values for scission and cross-linking ($G(S)$/$G(X)$) and β is a constant related to polymer structure. The difference in the two D_g values indicate that a large reduction in the average level of main chain scissions with respect to cross-links occurs in the presence of acetylene.

The experimental gel-dose curve (Figure 1) was analyzed using the $(gel)_{T_{max}}$ curve and the method described previously.[1−3] In steps of 0.02 gel fraction, $N_{CS,D}$ values were calculated, by dividing the interpolated experimental gel-dose (D) by the corresponding $(gel)_{T_{max}}$-dose required to produce the same gel fraction in the hypothetical absence of chain reactions, scissions, or cross-link redundancies. The resulting $N_{CS,D}$ values, plotted as a function of D (Figure 2), decay, similarly to those of the LLDPEs,[3] in what appears to be near second-order decay with respect to dose in excess that required for incipient gelation ($D' = D - D_g$). The initial increase in $N_{CS,D}$ is somewhat less than first order with respect to D'. Hence, the data points functionally fit the equation

$$N_{CS,D} = \frac{K_1 D'^{a}}{\{K_1 K_2 D'^{2a} + 1\}} \quad (6)$$

where K_1, K_2, and a are constants. The least-squares fitting parameters for eq 6 are given for the present i-PP (**3a**) and previous LLDPE results (**1v**, **1a**, and **2a**) (Table

Table 1. Atomistic Constants for $N_{CS,D}$ Parameters

polymer	LLDPE (**1v**)	LLDPE (**1a**)	LLDPE (**2a**)	i-PP 2400 (**3a**)
conditions	in vacuo	in C_2H_2	in C_2H_2	in C_2H_2
$M_{n,0}$/kg mol^{-1}	22.05	22.05	30.50	57.10
$(N_{CS,D})_{max}$	2.9	9.0	4.85	2.52
K_1/Gy^{-a}	3.75×10^{-3}	7.93×10^{-3}	3.50×10^{-3}	9.00×10^{-3}
K_2/Gy^{-a}	1.13×10^{-4}	2.30×10^{-5}	3.68×10^{-5}	3.54×10^{-4}
a	0.688	0.811	0.787	0.691
n_i (order of increase)	0.69	0.68	0.61	0.72
n_d (order of decrease)	2.57	2.12	2.52	2.41
decrease rate constant k_n/Gy	1.17×10^{-6}	1.78×10^{-6}	1.31×10^{-6}	7.45×10^{-6}

1). The order of increase (n_i) and decrease (n_d), and the decrease rate constant (k_n), were estimated from the initial ($1 - n_i$) and final gradients ($1 - n_d$) and the final intercept ($-\{\ln(k_n) + \ln(n - 1)\}$), respectively, of plots of $\ln(D)$ vs $\ln(N_{CS,D})$, assuming the nth order equation

$$(N_{CS,D})^{1-n} = (n - 1)k_n D \tag{7}$$

held, where $n = n_i$ and n_d, for the increasing and decreasing parts of the $N_{CS,D}$ vs dose plots (Figure 2). The orders and decay rate constants are also shown in Table 1. The nearly second-order decay kinetics of the microporous i-PP and the LLDPE samples arise because at increasingly higher doses radical−radical termination occurs more frequently. The increase in radical−radical termination reactions, with respect to the number of linear chain steps, observed as a function of total absorbed dose, is a result of increasing proximity. It must be remembered that many of the radicals do not react during the irradiation, only becoming available for reaction later at the annealing stage (135 °C). As far as the current study is concerned, this tends to produce the effect of the entire dose being absorbed or reacting, in one go, irrespective of the dose rate. It would also appear from Table 1 that, for the irradiations of both the LLDPEs (**1a**, **2a**) and the i-PP (**3a**) in acetylene, $(N_{CS,D})_{max}$ decreases with increasing $M_{n,0}$.

Calculations of $(N_{Xeff,D}/N_M)_{gel}$ were made on the i-PP data, using the $N_{CS,D}$ values in the following equation:

$$\left(\frac{N_{Xeff}}{N_M}\right)_{gel} = D\frac{G(R^\bullet)}{2}N_{CS,}DM_{n,0} \tag{8}$$

$G(R^\bullet)/2$ appears in this equation, because it takes two radicals to form a cross-link in the absence of chain reactions (eqs 2 and 3). The resulting interpolated and experimental gel fraction vs $(N_{Xeff,D}/N_M)_{gel}$ plots for the i-PP samples are shown (Figure 3) together with three plots from the previous LLDPEs. It can immediately be seen that the microporous i-PP (**3a**) (57.10 kg mol^{-1}, in acetylene) plots are almost identical to the LLDPE (**2a**) (30.50 kg mol^{-1}, in acetylene) plot,[2] which is also very close to the two LLDPE (**1v**, **1a**) (22.05 kg mol^{-1}, in vacuo and in acetylene) plots.[1] The deviation of the two LLDPE (**1v**, **1a**) (22.05 kg mol^{-1}) plots from the LLDPE (**2a**) (30.50 kg mol^{-1}) and microporous i-PP (**3a**) plots, from about 0.6 gel fraction onward, probably results from experimental errors in the gel fraction measurement. The results corroborate the previous idea that gel fraction vs $(N_{Xeff,D}/N_M)_{gel}$ curves derived from polyalkenes conform to a universal function, irrespective of $M_{n,0}$ (above some limiting size), or the irradiation and annealing conditions used to produce them.[2]

As for the LLDPE data sets, the i-PP data were functionally fitted to the following equation

$$g = \left(\frac{N_{Xeff,D}}{N_M}\right)_{gel}\Phi \tag{9}$$

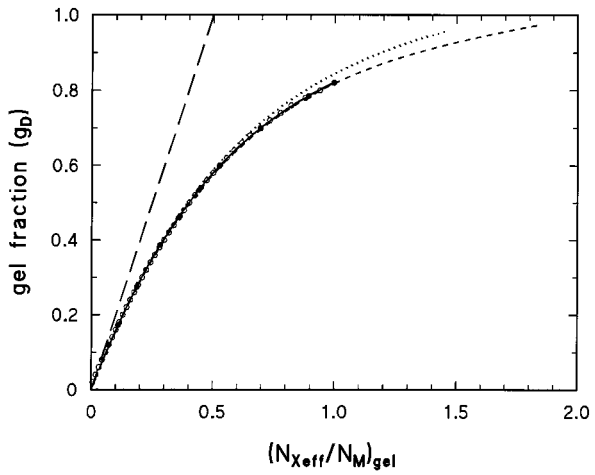

Figure 3. Gel fraction vs $(N_{Xeff,D}/N_M)_{gel}$ for i-PP (**3a**) ($M_{n,0}$ = 57.10 kg mol^{-1}, in C_2H_2) experimental data (●), interpolated data (○), and functional fit to interpolated data (—); LLDPE (**2a**) ($M_{n,0}$ = 30.50 kg mol^{-1}, in C_2H_2) (- -); LLDPE (**1v**, **1a**) ($M_{n,0}$ = 22.05 kg mol^{-1}, in vacuo and in C_2H_2) (···); and the hypothetical linear plot for $\Phi = 2$, or $g = 2$; $(N_{Xeff,D}/N_M)_{gel}$ (chains connected once only to one other chain with no redundancies) (— —).

Table 2. Atomistic Constants for Gel Fraction vs $(N_{Xeff}/N_M)_{Gel}$

polymer	LLDPE (**1v**)	LLDPE (**1a**)	LLDPE (**2a**)	i-PP 2400 (**3a**)
conditions	in vacuo	in C_2H_2	in C_2H_2	in C_2H_2
$M_{n,0}$/kg mol^{-1}	22.05	22.05	30.50	57.10
K_3	0.7105	0.6928	0.7135	0.7037
C	0.1612	0.1681	0.1494	0.1525

where Φ is the mean connectivity per "gel-effective" cross-link, over all gel-network regions

$$\Phi = 2\left\{K_3 \exp\left(-\left(\frac{N_{Xeff,D}}{N_M}\right)_{gel}\right) + C\right\} \tag{10}$$

yielding the least-squares constant fitting parameters for K_3 and C compared in Table 2. The K_3 and C data in Table 2 yield standard deviations of 7.95×10^{-3} and 7.35×10^{-3} respectively, for the mean values 0.705 and 0.158. This further demonstrates the universality of the gel fraction vs $(N_{Xeff,D}/N_M)_{gel}$ data obtained from the polyalkenes in this and the previous studies.

The difference between $(N_{Xeff,D}/N_M)_{gel}$ and $(N_{X,D}/N_M)_{rh}$ at gel fractions greater than 0.4 seen previously,[2,3] and described by eq 1 above, by implication arises from redundancies and the extra cross-links required to overcome the low level of scission processes that occur in the presence of acetylene. Initially, at low gel-fractions, the probability that a scission will effect the gel fraction is low, because it is unlikely that scissions and cross-links take place in the same chains, and even if they do there is further a low probability that this will affect large polymer chains. A scission in an uncross-linked chain has no effect on the sol fraction and hence, the gel fraction. At very high gel fractions there

is also a low probability that scissions will have an effect on the gel fraction, because the cut chains are increasingly more likely to be attached elsewhere through the network. However, at high gel fractions there is an increasingly low probability that scission fragments created earlier will be cross-linked back into the network, because the random nature of dose deposition creates large quantities of redundant cross-links. This explains why the gel-$(N_{X,D}/N_M)_{rh}$ curve initially is identical to the gel$-(N_{Xeff,D}/N_M)_{gel}$ curve, but later diverges as the power function of eq 1.

Eventually, it should be possible, by varying the scission probability (p(Sc)) and the number of real chain steps ($N_{RCS,D}$), to fit the gel data via our algorithm to the gel$-(N_{X,D}/N_M)_{rh}$ curve. This would facilitate simulation of both the "total" numbers of cross-links and scissions required to reproduce the rheological data.

2. Flory Stockmayer Analysis of Gel Fraction Curves. 2.1. General Theory. As described previously,[1] the analysis is based on the Flory−Stockmayer (F−S) treatment, of an RA_f (polyfunctional) self-polymerization.[15,16] The analysis is extended here to allow calculation of the number of "scission-free" reactions.

The fundamental assumptions implicit in the use of F−S theory are as follows: (i) intermolecular cross-linking reactions occur completely at random; (ii) no pre-gel intramolecular reaction occurs (no cross-links between reactive sites on the same molecule before the gel point); (iii) random post-gel intramolecular reactions (redundancies) in the gel molecules are allowed. The independent variable is the extent of reaction, p, where

$$p = \frac{\text{number of sites reacted}}{\text{total number of sites}} \tag{11}$$

For LLDPE, each methylene repeat unit constitutes a reactive "site", which can form a $-^{\bullet}CH-$ radical. For i-PP, however, the propylene repeat unit is defined as the reactive "site", capable of forming one radical. It is assumed that every radical formed gives rise to a cross-link and the effects of possible chain scission are ignored, thus providing a hypothetical "scission-free" model, in which p is related to the equivalent radiation dose as

$$D_{FS} = \frac{p}{G(R^{\bullet})M_{RU}} \tag{12}$$

where D_{FS} is the F−S dose that corresponds to an extent of reaction p, $G(R^{\bullet})$ is the radiation efficiency value of eqs 3 and 4, and M_{RU} is the mass of the repeat unit capable of forming one radical.

In contrast to the atomistic analysis presented earlier, where the number-average molecule is considered, F−S theory relates to the weight-average molecule. The number of reactive sites per weight-average molecule, or weight-average functionality, is given by

$$f_w = \frac{M_w}{M_{RU}} \tag{13}$$

where M_w is the weight-average molar mass of the sample before irradiation. In the cases under consideration here, for LLDPE (**1v** and **1a**) (M_n = 22.05 kg mol^{-1}),[2] M_w = 106 kg mol^{-1}, hence f_w = 7550; for LLDPE (**2a**) (M_n = 30.50 kg mol^{-1}),[2] M_w = 138 kg mol^{-1}, hence f_w = 9839; and for i-PP (**3a**) (M_n = 57.10 kg mol^{-1}) M_w = 471 kg mol^{-1}, hence f_w = 11214. These values are summarized in Table 3.

Table 3. F−S Constants for $N_{CS,D}$ Parameters

polymer	LLDPE (**1v**)	LLDPE (**1a**)	LLDPE (**2a**)	i-PP 2400 (**3a**)
conditions	in vacuo	in C_2H_2	in C_2H_2	in C_2H_2
$M_{n,0}$/kg mol^{-1}	22.05	22.05	30.50	57.10
$M_{w,0}$/kg mol^{-1}	106	106	138	471
fw	7550	7550	9839	11214
$(N_{CS,D})_{max} = N_{CS,D_g}$	2.8	9.4	3.4	2.0
n order of decrease	2.65	2.83	2.45	2.18
decrease rate k_n/Gy	1.20×10^{-5}	5.60×10^{-6}	1.18×10^{-5}	7.72×10^{-5}

The gel fraction (g) is calculated as a function of p using the method described previously.[16] Consistent with F−S statistics, the gel point is defined as the point at which a covalently linked network *first* occurs, giving the extent of reaction at gel (p_g) as

$$p_g = \frac{1}{(f_w - 1)} \tag{14}$$

Thus, the gel fraction is zero up to the gel point and then increases to a limiting value of 1 at complete reaction, at which point all the starting molecules are cross-linked to form a single, infinite "gel-molecule". However, the molecular structures of the cross-linked networks cannot be defined precisely, and g must be found theoretically, by calculating the complementary quantity, the unit fraction of sol (s), using the expression

$$g = 1 - s \tag{15}$$

s is found by summing over all the finite (defined) molecular species

$$s = \sum_{x=1}^{\infty} u_x \tag{16}$$

where u_x is the unit fraction of the species with degree of polymerization x. For an RA_f polymerization, u_x is given by

$$u_x = \frac{x(1-p)^2}{p} \frac{f[x(f-1)]!}{[x(f-2)+2]!\, x!} \beta^x \tag{17}$$

where $f = f_w$ and

$$\beta = p(1-p)^{(f-2)} \tag{18}$$

The combinatorial factor in eq 17 accounts for the number of distinct isomers of molecular species with defined structures of x units, i.e., those with $[x(f-2)+2]$ unreacted sites. Performing the summation in eq 16 yields the final expression for s, for an RA_f polymerization

$$s = \frac{(1-p)^2 p^*}{(1-p^*)^2 p} \tag{19}$$

where p^* is the lowest value of p which satisfies eq 18 for a given value of β. The factor β describes the relationship between the distributions of finite molecular species pre- and post-gel. p^*, β, s, and g are evaluated for different values of p and the known values of f_w. Importantly, g is obtainable as a function of p through eqs 15 and 19. Hence, for given values of g and p, D_{FS} can be calculated using eq 12.

2.2. Correlation of Gel Fraction Curves. Values of g were first converted to p and then D_{FS} using eqs

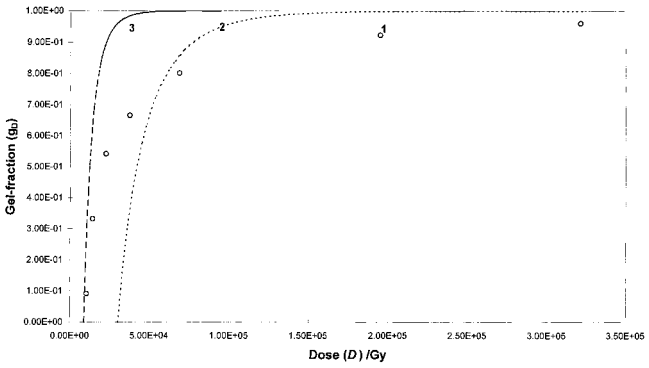

Figure 4. Gel-fraction vs dose for LLDPE (**2a**) ($M_{w,0} = 9839$) in acetylene, showing (1) the experimental data, (2) the F−S curve for $f_w = 9839$, produced via eqs 12 and 19, and (3) the "shifted F−S curve" produced using a constant factor N_{CS,D_g} (eq 21) applied to the entire dose range via eq 20.

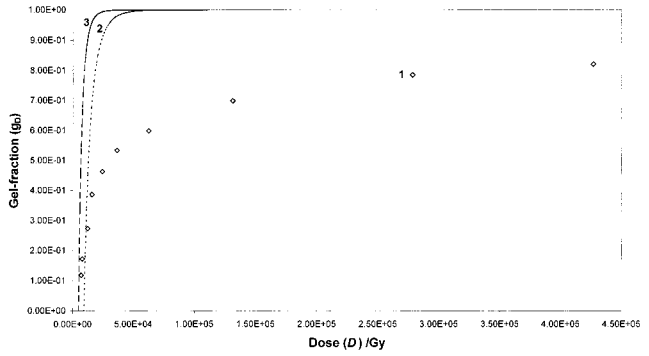

Figure 5. Gel-fraction vs dose plots for i-PP (**3a**) showing (1) the experimental data, (2) the F−S curve for $f_w = 11214$, produced via eqs 12, 15, and 19, and (3) the "shifted F−S curve" produced using constant N_{CS,D_g} (eq 21) applied to the entire dose range via eq 20.

15, 19, and 12. The resulting curves of gel fraction vs D_{FS} for LLDPE ($f_w = 9839$) and i-PP ($f_w = 11214$) are shown as curves 2 in Figures 4 and 5, together with the respective experimental gel fraction data (points 1). As shown previously,[16] for the results on LLDPE (**1**) in vacuo and in acetylene, the gel−D_{FS} curves are shifted in a positive direction along the dose axis, compared to the initial portion of the respective experimental data. Thus, because of the presence of the chain reactions, the $G(R^\bullet)$ values used in the F−S analysis (the same as those quoted in the atomistic analysis earlier) predict that gelation requires a higher dose than observed experimentally. This being the case, the experimental dose for a given gel fraction can be described in terms of p and the equivalent number of "gel-effective" chain steps per initiating radical ($N_{CS,D}$) by modifying eq 12 as follows:

$$D = \frac{p}{N_{CS,D_g}(R^\bullet)M_{RU}} = \frac{D_{FS}}{N_{CS,D}} \qquad (20)$$

The F−S gel fraction vs D_{FS} curves were shifted by a factor back along the dose axis, so that the predicted doses at the F−S gel points ($D_{FS,g}$) coincide with the experimental dose to incipient gelation (D_g). This was achieved by using a constant factor (N_{CS,D_g}), the number of "gel-effective" chain steps at the gel point, obtained by substituting D_g for D and p_g for p in eq 20, over the entire dose range, giving

$$N_{CS,D_g} = \frac{p_g}{D_g G(R^\bullet)M_{RU}} = \frac{D_{FS,g}}{D_g} \qquad (21)$$

As shown previously[1] for the LLDPE (**1**), the resulting shifted plots of gel fraction vs $D_{FS,g}$ (Figures 4 and 5 (curves 3)) do not fit the experimental data, because of the decay in $N_{CS,D}$ from the gel point onward. The values of $N_{CS,D}$ required to reproduce the experimental gel-fraction vs dose data were determined by rearranging eq 20 to give

$$N_{CS,D} = \frac{D_{FS}}{D} \qquad (22)$$

The results are shown in Figure 6, for all the results from the LLDPE (**1v** and **1a**), LLDPE (**2a**), and i-PP (**3a**) samples, where $N_{CS,D}$ is expressed as a function of D'. In all cases, the maximum value of $N_{CS,D}$ occurs at the gel-point ($D' = 0$, $N_{CS,D} = N_{CS,D_g}$), and these values of N_{CS,D_g} are given in Table 3.

It can be seen from Figure 6 and Table 3, that, for the experiments performed in acetylene, the N_{CS,D_g} value at $D' = 0$ decreases as $M_{n,0}$ increases from LLDPE (**1a**) to i-PP (**3a**). These trends are consistent with those from the atomistic analysis and with the smaller shifts in Figures 4 and 5 for LLDPE(**2a**) and i-PP (**3a**) compared with those for LLDPE (**1a**).[1]

At radiation doses beyond the gel point, the decrease in the number of chain-steps can be analyzed kinetically as a function of dose. If $N_{CS,D}$ is assumed to follow an nth-order decay after the gel-point, then

$$-\frac{d\{N_{CS,D}\}}{dD'} = k_n\{N_{CS,D}\}^n \qquad (23)$$

where k_n is the nth order rate constant with respect to D'. Integrating eq 23 with respect to D', from N_{CS,D_g} over the range of $N_{CS,D'}$, yields an expression for D':

$$k_n D' = \frac{1}{n-1}\{{N_{CS,D}}^{1-n} - {N_{CS,D_g}}^{1-n}\} \qquad (24)$$

In Figure 6, the decay curves shown were fitted using a least-squares method applied to eq 24, and the values of k_n and n obtained are listed in Table 3. The curves for LLDPE (**1v**) in vacuo, LLDPE (**2a**), in acetylene and i-PP (**3a**) in acetylene provide good representations of the results over the whole range of D'. Deviations are, however, observed at the higher doses for LLDPE (**1a**) irradiated in acetylene.

Finally, $N_{CS,D}$ and N_{CS,D_g} in eq 24 can be replaced by (D_{FS}/D) and ($D_{FS,g}/D_g$) using eqs 21 and 22. Then, for given gel fractions (g) and, hence, D_{FS}, values of D' (or D) can be calculated. This procedure essentially scales curves 2 in Figures 4 and 5 onto the experimental g vs D curves using the values of $N_{CS,D}$ shown in Figure 6. The resulting curves for LLDPE (**1v**, **1a**), LLDPE (**2a**), and i-PP (**3a**) are shown in Figure 7. They are seen to provide reasonable approximations to the experimental data, as they should because of the self-consistent procedure used. Again, the curve for the points from LLDPE (**1a**) irradiated in acetylene, show deviations at higher doses as a result of departure of $N_{CS,D}$ from nth-order kinetics with respect to D' (eq 24).

The relationship between g and the number of cross-links per molecule can be derived starting from the F−S

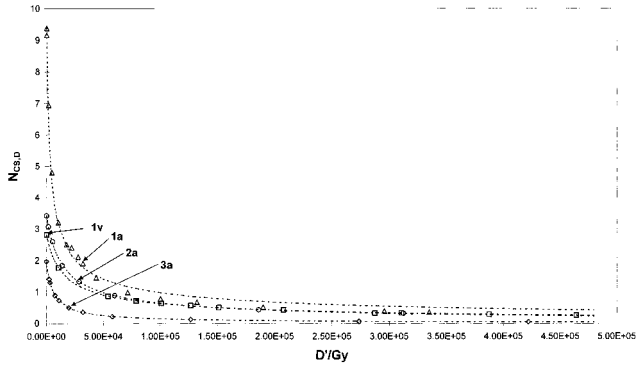

Figure 6. $N_{CS,D}$ (=D_{FS}/D) vs D' for LLDPE (**1v**) (f_w = 7550) in vacuo, LLDPE (**1a**) (f_w = 7550) in acetylene, LLDPE (**2a**) (f_w = 9839) in acetylene, and microporous i-PP (**3a**) (f_w = 11214) in acetylene.

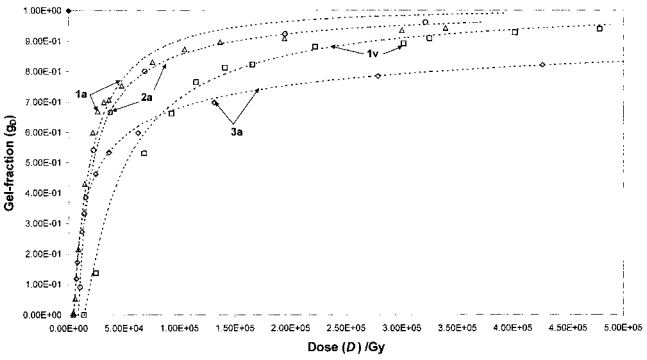

Figure 7. Experimental gel-fraction data fitted to eq 24 for LLDPE (**1v**) (f_w = 7550) in vacuo, LLDPE (**1a**) (f_w = 7550) in acetylene, LLDPE (**2a**) (f_w = 9839) in acetylene, and microporous i-PP (**3a**) (f_w = 11214) in acetylene.

gel-point condition eq 24, which for $f_w \gg 1$ may be rewritten

$$p_g f_w = 1 \tag{25}$$

Generally, pf_w is the number of "gel-effective" cross-linked units per weight-average molecule. Equation 25 shows this is equal to 1 at the gel point. Given that N_{Xeff} is the total number of units cross-linked over the initial N_M molecules, then, at any value of $p \geq p_g$

$$\left(\frac{N_{Xeff}}{N_M}\right)_{FS} = pf_w \tag{26}$$

Through eqs 15 and 19 and f_w, g is known as a function of p. Thus, in Figure 8, the universal theoretical curve of g as a function of $(N_{Xeff}/N_M)_{FS}$ is plotted using eq 26 to evaluate $(N_{Xeff}/N_M)_{FS}$. For the experimental data, using eqs 12, 13, and 20 for p, g and D_{FS} gives

$$\left(\frac{N_{Xeff}}{N_M}\right)_{FS} = D_{FS}G(R^{\bullet})M_W = DG(R^{\bullet})N_{CS,D}M_W \tag{27}$$

The experimental values of g are plotted in Figure 8 vs $(N_{Xeff}/N_M)_{FS}$ evaluated using eq 27. It can be seen that all of the experimental data points lie on or close to the "universal" curve, with LLDPE (**1a**) points again showing some deviation. The universal behavior is consistent with similar observations from the atomistic analysis.

Conclusions

This study shows that both the atomistic analysis and F−S theory are successful in fitting experimental gel-

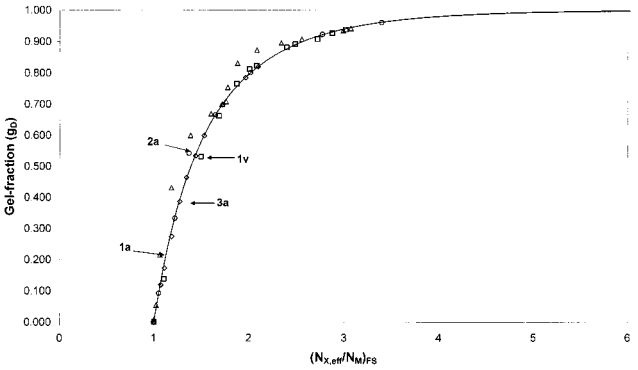

Figure 8. Gel-fraction vs number of "gel-effective" reactions per molecule from eq 27 for LLDPE (**1v**) (f_w = 7550) in vacuo, LLDPE (**1a**) (f_w = 7550) in acetylene, LLDPE (**2a**) (f_w = 9839) in acetylene, and microporous i-PP (**3a**) (f_w = 11214) in acetylene. The solid curve shows the universal F−S behavior (eq 26).

fraction data from an irradiated and annealed i-PP ($M_{n,0}$ = 57.10 kg mol^{-1}, $M_{w,0}$ = 471 kg mol^{-1}) in acetylene, when a variable is incorporated which represents the number of hypothetical "gel-effective" chain steps ($N_{CS,D}$) per radical generated at a given radiation dose. The presence of nonbranching chain reactions was demonstrated atomistically by the experimental gel fraction vs dose curve being initially much greater than the maximum possible gel fraction curve ($(gel)_{T_{max}}$), computationally calculated using spatial data from an MSI amorphous macrocell, to model 2.95 × 10^6 atoms, assuming that all radicals underwent immediate terminating cross-linking reactions. These results are in keeping with two similar previous studies on data from two different LLDPEs ($M_{n,0}$ = 22.05 kg mol^{-1}, $M_{w,0}$ = 106 kg mol^{-1} and $M_{n,0}$ = 30.50 kg mol^{-1}, $M_{w,0}$ = 138 kg mol^{-1}, respectively),[1−3] the former of which had been conducted both in vacuo and in acetylene. Considering the differences in the approaches of the atomistic and F−S methods of analyses, they complement each other well. The maximum numbers of "gel-effective" chain steps ($(N_{CS,D})_{max}$), derived by the two methods for all the polymers in all three studies, are in close agreement. So too are the *n*th-order decreases of $N_{CS,D}$, with respect to dose, with the exception of the LLDPE (**1a**) ($M_{n,0}$ = 22.05 kg mol^{-1}, $M_{w,0}$ = 106 kg mol^{-1}) irradiated and annealed in acetylene. The *n*th-order decrease rate constants, generated by the two different methods of analyses, differ by an order of magnitude, again with the exception of LLDPE (**1a**) (in acetylene), but follow the same trends. The F−S *n*th-order decrease rate constants are slower, because the F−S technique does not measure $N_{CS,D}$ prior to the gel-point and uses relative dose D'. The techniques show that for equivalent conditions in acetylene, $(N_{CS,D})_{max}$, and N_{CS,D_g} (F−S), decrease with increasing preirradiated molecular weight (LLDPE (**1a**) to i-PP (**3a**)).

Both the atomistic and F−S analyses of the i-PP 2400 gel fractions in this study, and those of the LLDPEs from the previously associated studies,[1,2] corroborate the earlier idea[2] that gel fraction vs $(N_{Xeff,D}/N_M)_{gel}$ curves derived from polyalkenes conform to a universal function, irrespective of the initial degree of polymerization (above some limiting size) or the irradiation and annealing conditions used to produce them. For the F−S method, the size of initial preirradiated polymer chains was described as a weight-average functionality, because F−S theory relates to the weight-average mol-

ecule. For the atomistic method, the preirradiated chain size was described as a number-average functionality.

It can be concluded that both the atomistic and F−S approaches afford simple and convenient methods of analysis of radiation-induced gel fractions in polyalkenes, providing additional insight as to the composition of the irradiated polymers. As described earlier, this work paves the way for the simulation and characterization of gel fraction data in terms of "total" numbers of permanent cross-links and chain scissions. This could be facilitated by varying the scission probability (p(Sc)) and the numbers of dose-related chain steps required to simultaneously reproduce both the gel fraction vs dose curves and the curves of gel fraction vs numbers of rheologically determined cross-links per initial chain.

Acknowledgment. The support of EPSRC Grants GR/L/62306 and GR/L/66649 to the University of Leeds and the Polymer Science and Technology Group, Manchester Materials Science Centre, are gratefully acknowledged. The project is also indebted to the Hoechst-Celanese Corp. for providing i-PP microporous membrane films (CELGARD 2400).

References and Notes

(1) Jones, R. A.; Ward, I. M.; Taylor, D. J. R.; Stepto, R. F. T. Reactions of amorphous PE radical-pairs in vacuo and in acetylene: a comparison of gel fraction data with Flory-Stockmayer and atomistic modelling analyses. *Polymer* **1996**, *37*, 3643−3657.

(2) Jones, R. A.; Groves, D. J.; Ward, I. M. An Investigation into the Relationship between Gel-effective' and Total Numbers of Cross-links in Irradiated LLDPE. *Polym. Int.* **1997**, *44*, 300−310.

(3) Jones, R. A.; Groves, D. J.; Ward, I. M.; Taylor, D. J. R.; Stepto, R. F. T. Gel Fractions and Chain Reactions in Irradiated Polyethylenes. *Nucl. Instrum. Methods Phys. Res., B* **1999**, *151*, 213−217. (Also in: *Ionizing Radiation and Polymers; Proc. 3rd Int. Symp. Ionizing Radiation and Polymers* (*IRaP '98*); Knolle, W., Trautmann, C., Eds.; North-Holland: The Netherlands, 1999; pp 213−217.)

(4) Jones, R. A.; Salmon, G. A.; Ward, I. M. Radiation Induced Cross-linking of Polyethylene in the Presence of Acetylene: A Gel Fraction, UV−Vis and ESR Spectroscopy Study. *J. Polym. Sci., Part B: Polym. Phys.* **1993**, *31*, 807−819.

(5) Molecular Simulations Incorporated., 9685 Scranton Road, San Diego, CA 92121−277.

(6) Jones, R. A.; Taylor, D. J. R.; Stepto, R. F. T.; Ward, I. M. Computer Modelling of the Formation of Radical Pairs in Amorphous High Density Polyethylene (HDPE). *J. Polym. Sci., Part B: Polym. Phys.* **1996**, *34*, 901−908.

(7) Patel, G. N.; Keller, A. Crystallinity and the Effect of Ionizing Radiation in Polyethylene. II. Crosslinking in Chain-Folded Single Crystals. *J. Polym. Sci., Part B: Polym. Phys. Ed.* **1975**, *13*, 323−331.

(8) Jones, R. A. A note on H-atom transfer and alkyl radical migration in polyethylene crystallites: MNDO saddle-point energies in a model *n*-heptane crystal. *Radiat. Phys. Chem.* **1998**, *53*, 19−23.

(9) Jones, R. A.; Taylor, D. J. R.; Cail, J. I.; Stepto, R. F. T.; Ward, I. M. Atomistic Modelling of the Formation of Radical Pairs in Amorphous Poly(propylene). *Macromolecules* **1999**, *32*, 8350−8355.

(10) Ohnishi, S. ESR Study of the Radiation Chemical Process in Polyethylene. *Bull. Chem. Soc. Jpn.* **1962**, *35*, 254−259.

(11) Shioji, Y.; Ohnishi, S.; Nitta, I. *Annu. Rep. JARRP* **1960**, *2*, 253.

(12) Ichikawa, T.; Kawahara, S.; Yoshida, H. Local Distribution of Alkyl Radicals in γ-Irradiated Polyethylene Studied by Electron Spin−Echo Method. *Radiat. Phys. Chem.* **1985**, *26*, 731−737.

(13) Veselovskii, R. A.; Leshchenko, S. S.; Karpov, V. L. *Polym., Sci. USSR* **1968**, *10*, 881.

(14) Jones, R. A. A Synopsis of of Empirical Gel Fraction Analytical Methods: Application of the Wanxi Equation to Polyethylenes Irradiated in Vacuo and in the Presence of Acetylene. *J. Polym. Sci., Part B: Polym. Phys.* **1994**, *32*, 2049−2053.

(15) Stockmayer, W. H. *J. Polym. Sci.* **1953**, *11*, 424.

(16) Stepto, R. F. T. In *Comprehensive Polymer Science*, 1st Suppl. ed.; Aggarwal, S. L., Russo, S., Eds.; Pergamon Press: Oxford, England, 1992; Chapter 10.

MA000701G